

SLOW VISCOUS MOTION OF A SOLID PARTICLE
IN A SPHERICAL CAVITY

A. Sellier

LadHyX. Ecole Polytechnique. France.

e-mail: sellier@ladhyx.polytechnique.fr

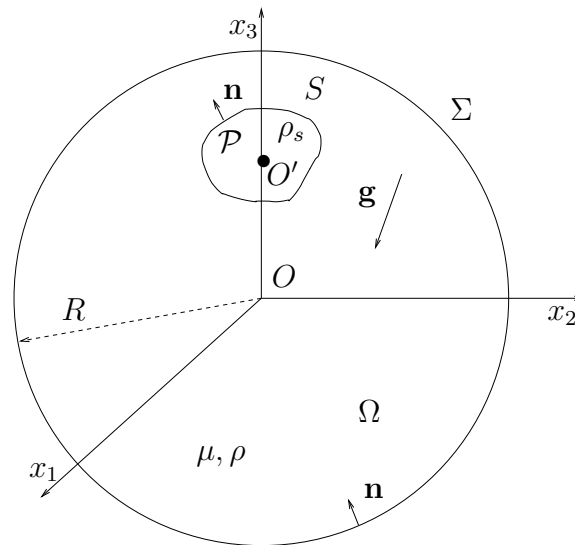
Seminar at IPPT

Warsaw, 16 November 2011

Outline

- 1) Addressed problem and assumptions
- 2) Key issues and available literature
- 3) Boundary approach and suitable Green tensor
- 4) Numerical implementation and comparisons
- 5) Numerical results for a non-spherical particle
- 6) Concluding remarks

Addressed problem



- A **Newtonian** liquid (ρ, μ) . Applied uniform gravity field \mathbf{g}
- The liquid is **confined by a solid and motionless cavity** Σ with attached Cartesian coordinates (O, x_1, x_2, x_3)
- A **solid arbitrary-shaped** particle \mathcal{P} with center of mass O' , uniform density ρ_s and smooth surface S with \mathbf{n} the unit outward normal
- The particle translates at \mathbf{U} (velocity of O') and rotates at \mathbf{W}

Basic issues

Experienced surface traction \mathbf{f} on S ?

Resulting hydrodynamic force \mathbf{F} and torque $\mathbf{\Gamma}$ (about O') on \mathcal{P} ?

Assumptions and governing equations

- The particle and its rigid-body motion (\mathbf{U} , \mathbf{W}) have length and velocity scales a and V .
- Assuming that $Re = \rho V a / \mu \ll 1$ one neglects inertia effects and obtains a quasi-steady flow (\mathbf{u} , $p + \rho \mathbf{g} \cdot \mathbf{x}$) in the liquid domain Ω

Creeping steady flow

$$\mu \nabla^2 \mathbf{u} = \nabla p \quad \text{and} \quad \nabla \cdot \mathbf{u} = 0 \quad \text{in } \Omega,$$

$$\mathbf{u} = \mathbf{0} \quad \text{on } \Sigma,$$

$$\mathbf{u} = \mathbf{U} + \mathbf{W} \wedge \mathbf{x}' \quad \text{on } S \quad \text{with} \quad \mathbf{x}' = \mathbf{O}'\mathbf{M}$$

Introducing the stress tensor $\boldsymbol{\sigma}$ such that $\sigma_{ij} = -p\delta_{ij} + \mu(u_{i,j} + u_{j,i})$, one looks at

$$\mathbf{f} = \boldsymbol{\sigma} \cdot \mathbf{n} \quad \text{on } S,$$

$$\mathbf{F} = \int_S \mathbf{f} dS, \quad \boldsymbol{\Gamma} = \int_S \mathbf{x}' \wedge \mathbf{f} dS$$

Two basic Problems

- Problem 1: (\mathbf{U} , \mathbf{W}) prescribed. Evaluation of \mathbf{F} and $\boldsymbol{\Gamma}$?
- Problem 2: freely-suspended particle \mathcal{P} with volume \mathcal{V} . Obtain (\mathbf{U} , \mathbf{W}) by enforcing

$$\mathbf{F} = (\rho - \rho_s) \mathcal{V} \mathbf{g}, \quad \boldsymbol{\Gamma} = \mathbf{0}$$

Auxiliary Stokes flows and key surface tractions

- $(\mathbf{u}_t^{(i)}, p_t^{(i)})$ and $(\mathbf{u}_r^{(i)}, p_r^{(i)})$ for $i = 1, 2, 3$. Stokes flows with $\mathbf{u}_t^{(i)} = \mathbf{u}_r^{(i)} = \mathbf{0}$ on Σ , $\mathbf{u}_t^{(i)} = \mathbf{e}_i$ and $\mathbf{u}_r^{(i)} = \mathbf{e}_i \wedge \mathbf{x}'$ on S
 - Resulting surface tractions $\mathbf{f}_t^{(i)}$ and $\mathbf{f}_r^{(i)}$ on S

Use for Problem 1

$$\mathbf{F} = -\mu\{\mathbf{A}_t \cdot \mathbf{U} + \mathbf{B}_t \cdot \mathbf{W}\}, \quad \mathbf{\Gamma} = -\mu\{\mathbf{A}_r \cdot \mathbf{U} + \mathbf{B}_r \cdot \mathbf{W}\}$$

$$-\mu A_L^{i,j} = \int_S \mathbf{f}_L^{(i)} \cdot \mathbf{e}_j dS, \quad -\mu B_L^{i,j} = \int_S (\mathbf{x}' \wedge \mathbf{f}_L^{(i)}) \cdot \mathbf{e}_j dS$$

Use for Problem 2

The rigid-body migration (\mathbf{U}, \mathbf{W}) is obtained by solving

$$\mu\{\mathbf{A}_t \cdot \mathbf{U} + \mathbf{B}_t \cdot \mathbf{W}\} = (\rho_s - \rho)\mathcal{V}\mathbf{g}$$

$$\mu\{\mathbf{A}_r \cdot \mathbf{U} + \mathbf{B}_r \cdot \mathbf{W}\} = \mathbf{0}$$

- Well-posed linear system
- Unique solution (\mathbf{U}, \mathbf{W})

Available literature?

- **Restricted** to a **spherical** particle!
- Case of a **translating** sphere located at the cavity center
 - Cunningham (1910), Williams (1915)
by obtaining the stream function (**exact** solution)
- Case of a sphere **not** located at the cavity center
 - Use of **bipolar coordinates** (well adapted to the fluid domain geometry)
 - Jeffery (1915), Stimson & Jeffery (1926), O'Neill & Majumdar (1970a, 1970b)
 - **recently**: accurate calculations by Jones (2008)
- **Merits**
 - very accurate solution (if carefully implemented)
 - able to deal with small sphere-cavity gaps!
 - provides very nice benchmark tests for other methods to be developed
- **Drawbacks**
 - cumbersome approach (tricky analytical manipulations)
 - provides the net force \mathbf{F} and torque $\mathbf{\Gamma}$ but still uneasy to calculate the surface tractions $\mathbf{f}_t^{(i)}$ and $\mathbf{f}_r^{(i)}$ on S
 - **not possible** to cope with one non-spherical particle
or with several particles!

Quite different boundary approach

Green tensors

- **y** source point or pole in the entire domain $\mathcal{D} = \Omega \cup \mathcal{P}$
- **x** observation point. For $j = 1, 2, 3$ one introduces a Stokes flows $(\mathbf{v}^{(j)}, p^{(j)})$,

$$\mu \nabla^2 \mathbf{v}^{(j)} = \nabla p^{(j)} - \delta_{3d}(\mathbf{x} - \mathbf{y}) \mathbf{e}_j, \quad \nabla \cdot \mathbf{v}^{(j)} = 0 \quad \text{in } \mathcal{D}$$

- Resulting Green tensor \mathbf{G} with Cartesian components

$$G_{kj}(\mathbf{x}, \mathbf{y}) = \mathbf{v}^{(j)}(\mathbf{x}, \mathbf{y}) \cdot \mathbf{e}_k$$

Remark, examples

- A Green tensor: not unique (no prescribed boundary conditions)
- Widely-employed free-space Green tensor \mathbf{G}^∞ such that

$$8\pi\mu G_{kj}^\infty(\mathbf{x}, \mathbf{y}) = \frac{\delta_{kj}}{|\mathbf{x} - \mathbf{y}|} + \frac{[(\mathbf{x} - \mathbf{y}) \cdot \mathbf{e}_j][(\mathbf{x} - \mathbf{y}) \cdot \mathbf{e}_k]}{|\mathbf{x} - \mathbf{y}|^3}$$

- Specific Green tensor \mathbf{G}^c for the given cavity Σ :

$$G_{jk}^c(\mathbf{x}, \mathbf{y}) = 0 \quad \text{for } \mathbf{x} \text{ on } \Sigma$$

Relevant integral representations and boundary-integral equations

- One looks at $\mathbf{f} = f_k \mathbf{e}_k$ on S for $\mathbf{u} = \mathbf{U} + \boldsymbol{\Omega} \wedge \mathbf{x}'$ on S
- Due to this velocity boundary condition, one gets a single-layer integral representation

$$[\mathbf{u} \cdot \mathbf{e}_j](\mathbf{x}) = - \int_{S \cup \Sigma} f_k(\mathbf{y}) G_{kj}(\mathbf{y}, \mathbf{x}) dS(\mathbf{y}) \quad \text{for } \mathbf{x} \text{ in } \Omega \cup S; j = 1, 2, 3.$$

(Here \mathbf{x} is the pole)

- Associated Fredholm boundary-integral equation of the first kind

$$[\mathbf{U} + \boldsymbol{\Omega} \wedge \mathbf{x}'] \cdot \mathbf{e}_j = - \int_{S \cup \Sigma} f_k(\mathbf{y}) G_{kj}(\mathbf{y}, \mathbf{x}) dS(\mathbf{y}) \quad \text{for } \mathbf{x} \text{ on } S; j = 1, 2, 3.$$

(solution unique up to $c\mathbf{n}$ with c constant)

- Valid for any Green tensor \mathbf{G} !
- Because $G_{jk}^c(\mathbf{y}, \mathbf{x}) = 0$ for \mathbf{y} on Σ , one replaces $S \cup \Sigma$ with S in the above integrals!
 - Additional general property: $G_{jk}^c(\mathbf{x}, \mathbf{y}) = G_{kj}^c(\mathbf{y}, \mathbf{x})$
under the condition $G_{jk}^c(\mathbf{x}, \mathbf{y}) = 0$ on Σ

Green tensor G^c for the spherical cavity

Obtained (in a different form not suitable for numerics) by Oseen 1927!

- Pole \mathbf{y} and observation point \mathbf{x} .

$$\mathbf{y}' = \frac{R^2 \mathbf{y}}{|\mathbf{y}|^2}, \quad \mathbf{t} = \frac{\mathbf{y}}{|\mathbf{y}|}, \quad \mathbf{a} = \mathbf{x} - (\mathbf{x} \cdot \mathbf{t}) \mathbf{t}, \quad \mathbf{h} = \frac{|\mathbf{y}|}{R} (\mathbf{x} - \mathbf{y}'), \quad h = |\mathbf{h}|$$

$$\begin{aligned} G_{jk}^c(\mathbf{x}, \mathbf{y}) = & G_{jk}^\infty(\mathbf{x}, \mathbf{y}) - \frac{\delta_{jk}}{h} - \frac{(\mathbf{x} \cdot \mathbf{e}_j)(\mathbf{x} \cdot \mathbf{e}_k)}{h^3} + \frac{(\mathbf{t} \cdot \mathbf{e}_j)(\mathbf{t} \cdot \mathbf{e}_k)}{h} \left[\frac{|\mathbf{x}|^2}{h^2} - 1 \right] \\ & - \left[\frac{2|\mathbf{y}| \mathbf{t} \cdot \mathbf{x}}{h^3} \right] (\mathbf{t} \cdot \mathbf{e}_j)(\mathbf{t} \cdot \mathbf{e}_k) + |\mathbf{y}| \left[\frac{(\mathbf{t} \cdot \mathbf{e}_j)(\mathbf{x} \cdot \mathbf{e}_k) + (\mathbf{t} \cdot \mathbf{e}_k)(\mathbf{x} \cdot \mathbf{e}_j)}{h^3} \right] \\ & - \frac{[|\mathbf{x}|^2 - R^2][|\mathbf{y}|^2 - R^2]}{2} \left\{ \frac{\delta_{jk}}{R^3 h^3} - \frac{3}{R^2} \left[\frac{(\mathbf{h} \cdot \mathbf{e}_j)(\mathbf{h} \cdot \mathbf{e}_k)}{h^5} \right] \right. \\ & - 2 \frac{\mathbf{t} \cdot \mathbf{e}_k}{R^2} \left[\frac{\mathbf{t} \cdot \mathbf{e}_j}{h^3} - \frac{3(\mathbf{h} \cdot \mathbf{e}_j)(\mathbf{h} \cdot \mathbf{t})}{h^5} \right] + \frac{3E}{R^4 h} [\delta_{jk} - (\mathbf{t} \cdot \mathbf{e}_k)(\mathbf{t} \cdot \mathbf{e}_j)] \\ & \left. + \frac{3\mathbf{a} \cdot \mathbf{e}_k}{R} \left[-\frac{E}{R^3 h} \left\{ \frac{|\mathbf{y}| \mathbf{h} \cdot \mathbf{e}_j}{R h^2} + \frac{2\mathbf{a} \cdot \mathbf{e}_j}{|\mathbf{a}|^2} \right\} + \frac{\mathbf{E} \cdot \mathbf{e}_j}{R^4 h^2 [|\mathbf{x}|_+^+ (\mathbf{x} \cdot \mathbf{t})]} + \mathbf{a} \cdot \mathbf{e}_j \left[\frac{(2R^2)_+^+ |\mathbf{y}| |\mathbf{x}|}{R^4 h^2 |\mathbf{a}|^2} \right] \right\} \end{aligned}$$

$$\mathbf{E} = \left\{ |\mathbf{x}|_+^+ \frac{2R^2 \mathbf{x} \cdot \mathbf{t}}{R^2 + R h_+^- |\mathbf{x}| |\mathbf{y}|} \right\} / \{ |\mathbf{x}|_+^+ \mathbf{x} \cdot \mathbf{t} \}, \quad \mathbf{E} = \left\{ |\mathbf{y}| \mathbf{x} + [|\mathbf{y}| |\mathbf{x}|_+^+ (1_+^- 2) R^2] \mathbf{t}_+^{+2} \left[\frac{2R^2 |\mathbf{y}| |\mathbf{x} + [R^3 h_+^- R^2 |\mathbf{y}| |\mathbf{x}|] \mathbf{t}}{R^2 + R h_+^- |\mathbf{y}| |\mathbf{x}|} \right] \right\}$$

with upperscripts or subscripts for $\mathbf{x} \cdot \mathbf{t} \geq 0$ or $\mathbf{x} \cdot \mathbf{t} < 0$, respectively

Numerical strategy

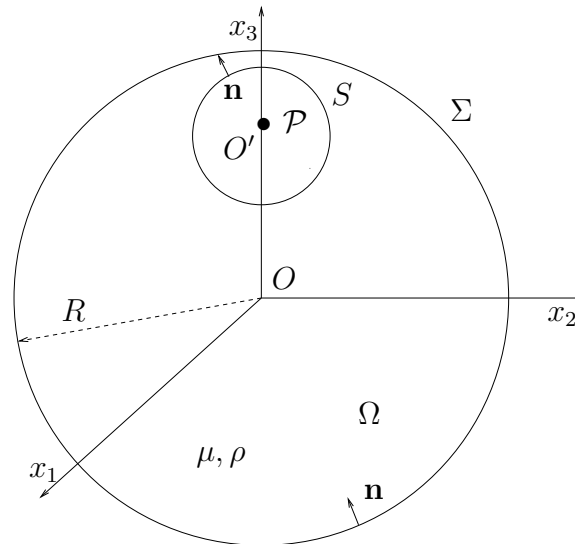
- Isoparametric triangular curvilinear Boundary Elements on S and, if needed, on the cavity Σ
- Discretize each boundary-integral equation. This requires to accurately deal with the case of a source \mathbf{x} on a boundary element (a refined treatment is needed with the use of local polar coordinates)
 - Solve each resulting linear systems $AX = Y$ by Gaussian elimination
- The use of \mathbf{G}^c permits one to solely mesh the particle's surface (worth for a large cavity)

Benchmarks are needed!

- As seen before, \mathbf{G}^c is available for a spherical cavity
- Comparisons with both analytical and numerical results for a spherical particle (previously-mentioned literature)
 - Sphere located or not located at the cavity center

Case of a spherical particle

Adopted notations



- A **spherical** cavity with center O and radius R
- A **spherical** particle with radius a and center O'
 - $\mathbf{OO}' = d\mathbf{e}_3$ and $0 \leq d < R - a$
 - $R - (d + a)$ is the **sphere-cavity gap**
- Normalized sphere-cavity gap $\eta = (R - d - a)/a$

Numerical comparisons for a sphere located at the cavity center

- Here $O = O'$ and $d = 0$. Sphere with radius $a < R$ translating at the velocity \mathbf{e}_i .

$$\mathbf{F} = -6\pi\mu ac(a/R)\mathbf{e}_i, \quad \mathbf{\Gamma} = \mathbf{0}$$

- Analytical formula for the occurring dimensionless resistance coefficient c

$$c(\beta) = \frac{1 - \beta^5}{1 - \frac{9\beta}{4} + \frac{5\beta^3}{2} - \frac{9\beta^5}{4} + \beta^6}, \quad \beta = a/R < 1.$$

- A $N - node$ mesh on the sphere and, if needed, 1058 nodal points on the cavity Σ

Two computed values of the above coefficient c

- c_s : using the Green \mathbf{G}^∞ and putting Stokeslets on both S and Σ
 - c_c : using the Green tensor \mathbf{G}^c and Stokeslets on S
 - Notation: $\Delta c_l = |c_l/c - 1|$

A translating sphere located at the cavity center

N	R/a	c_s	Δc_s	c_c	Δc_c
74	1.1	3258.137	1.00613	2097.155	0.29128
242	1.1	2124.983	0.30842	1949.547	0.01030
1058	1.1	1777.331	0.09436	1676.260	0.00353
exact	1.1	1624.089	0	1624.089	0
74	2.	7.223525	0.00968	7.218993	0.01030
242	2.	7.289179	0.00068	7.284937	0.00126
1058	2.	7.297493	0.00046	7.293273	0.00012
exact	2.	7.294118	0	7.294118	0
74	5.	1.749799	0.00344	1.749640	0.00353
242	5.	1.755232	0.00035	1.755073	0.00044
1058	5.	1.755937	0.00005	1.755777	0.00004
exact	5.	1.755845	0	1.755845	0

Computed quantities c_s , Δc_s , c_c and Δc_c
versus the number N of collocation points on S

Arbitrarily-located sphere

- Here $\mathbf{OO}' = d\mathbf{e}_3$ with $0 \leq d < R - a$.

For **symmetry reasons** one confines the attention to four cases.

- (i) A sphere translating at the velocity \mathbf{e}_1 : $\mathbf{F} = -6\pi\mu a c_1 \mathbf{e}_1$ and $\mathbf{\Gamma} = 8\pi\mu a^2 s \mathbf{e}_2$
 - (ii) A sphere translating at the velocity \mathbf{e}_3 : $\mathbf{F} = -6\pi\mu a c_3 \mathbf{e}_3$ and $\mathbf{\Gamma} = \mathbf{0}$
- (iii) A sphere rotating at the velocity \mathbf{e}_1 : $\mathbf{F} = -8\pi\mu a^2 s \mathbf{e}_2$ and $\mathbf{\Gamma} = -8\pi\mu a^3 t_1 \mathbf{e}_1$
 - (iv) A sphere rotating at the velocity \mathbf{e}_3 : $\mathbf{F} = \mathbf{0}$ and $\mathbf{\Gamma} = -8\pi\mu a^3 t_3 \mathbf{e}_3$

Comparisons for the computed coefficients c_1, c_3, t_1, t_3 and s

- Accurate computations obtained elsewhere by using the bipolar coordinates (Jones 2008, here **labelled Jones in each reported table**)
- $R = 4a$ and two values of the normalized gap $\eta = (R - d - a)/a$ are selected:
 $\eta = 0.5$ and $\eta = 0.1$ (small sphere-cavity gap).
- 4098 nodal points are put on the cavity Σ when using the Green tensor \mathbf{G}^∞

Comparisons for a sphere
not located at the cavity center
with $\eta = (R - d - a)/a = 0.5$

N	Method	c_1	c_3	t_1	t_3	s
74	\mathbf{G}^∞	2.6330	4.6730	1.1640	1.0789	0.11870
74	\mathbf{G}^c	2.6327	4.6714	1.1639	1.0789	0.11861
242	\mathbf{G}^∞	2.6473	4.7107	1.1639	1.0755	0.11927
242	\mathbf{G}^c	2.6471	4.7090	1.1639	1.0755	0.11920
1058	\mathbf{G}^∞	2.6488	4.7144	1.1639	1.0755	0.11938
1058	\mathbf{G}^c	2.6486	4.7127	1.1639	1.0755	0.11932
Jones	Bipolar	2.6487	4.7131	1.1639	1.0755	0.11933

Comparisons for a sphere
not located at the cavity center
with $\eta = (R - d - a)/a = 0.1$

N	Method	c_1	c_3	t_1	t_3	s
74	\mathbf{G}^∞	3.9016	15.552	1.6065	1.1960	0.20206
74	\mathbf{G}^c	3.9009	15.413	1.6052	1.1960	0.20138
242	\mathbf{G}^∞	3.9273	18.886	1.6145	1.1939	0.19108
242	\mathbf{G}^c	3.9237	18.636	1.6134	1.1938	0.19001
1058	\mathbf{G}^∞	3.9159	18.832	1.6171	1.1945	0.18494
1058	\mathbf{G}^c	3.9121	18.711	1.6160	1.1945	0.18353
Jones	Bipolar	3.9121	18.674	1.6163	1.1945	0.18344

Numerical results for a non-spherical particle

- Ellipsoid with semi-axis (a_1, a_2, a_3) and surface admitting the equation

$$(x_1/a_1)^2 + (x_2/a_2)^2 + ([x_3 - d]/a_3)^2 = 1$$

- Ellipsoid-cavity **normalized separation parameter** λ with

$$0 < \lambda = d/a_3 < (R - a_3)/a_3$$

- 8 **friction coefficients** c_i, t_i, s_1 and s_2 such that

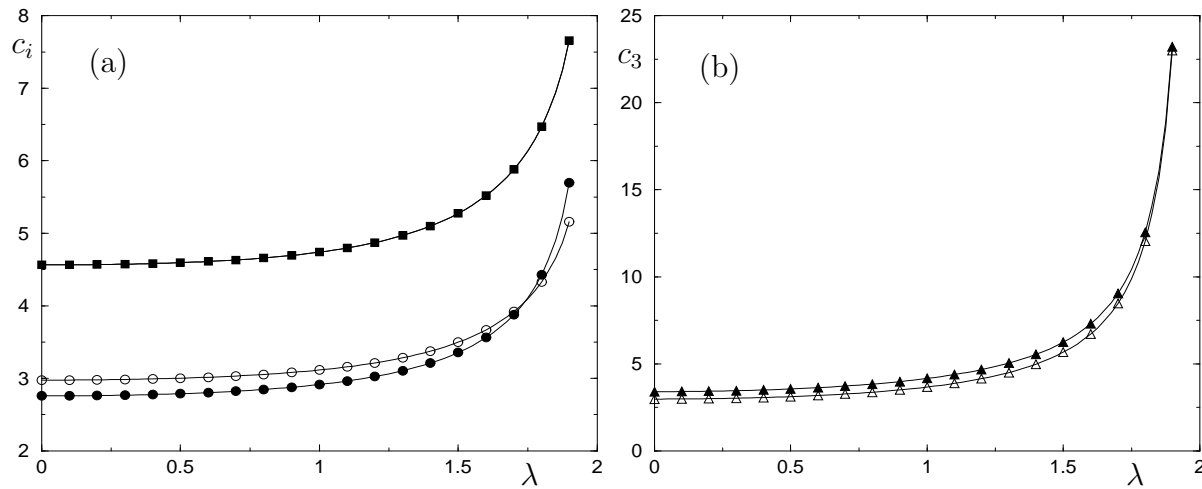
$$\begin{aligned}\mathbf{A}_T^{(i)} &= 6\pi\mu a_3 c_i \mathbf{e}_i, & \mathbf{B}_R^{(i)} &= 8\pi\mu a_3^3 t_i \mathbf{e}_i, \\ \mathbf{B}_T^{(1)} &= -8\pi\mu a_3^2 s_1 \mathbf{e}_2, & \mathbf{B}_T^{(2)} &= 8\pi\mu a_3^2 s_2 \mathbf{e}_1, & \mathbf{B}_T^{(3)} &= \mathbf{0}, \\ \mathbf{A}_R^{(1)} &= 8\pi\mu a_3^2 s_2 \mathbf{e}_2, & \mathbf{A}_R^{(2)} &= -8\pi\mu a_3^2 s_1 \mathbf{e}_1, & \mathbf{A}_R^{(3)} &= \mathbf{0}\end{aligned}$$

Comparisons for two selected ellipsoids

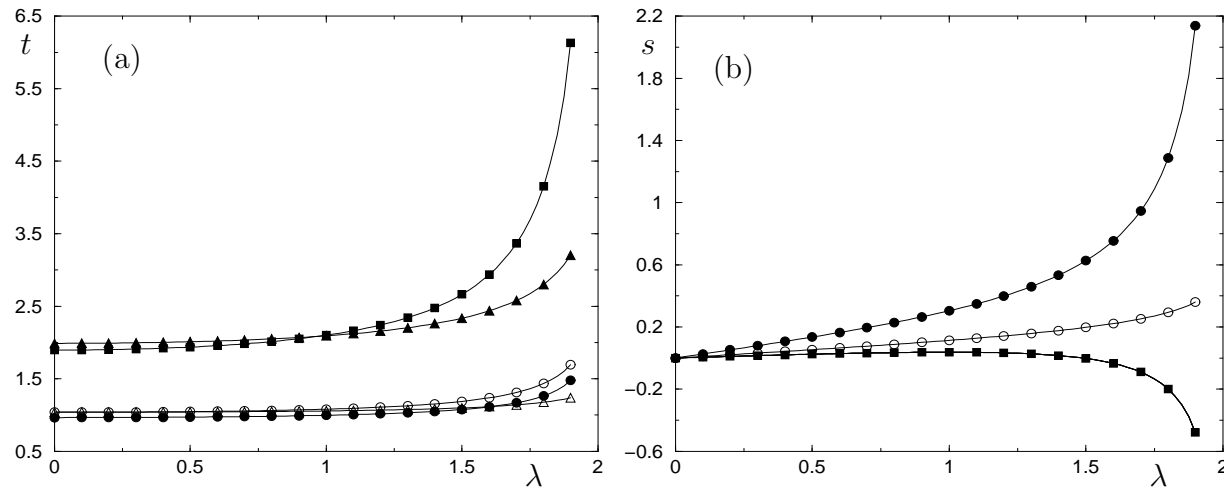
- A sphere with radius a_3 (clear symbols)
 - The ellipsoid $a_1 = 5a_3/3, a_2 = 0.6a_3$
having **the same volume as the sphere** (filled symbols)

Friction coefficients

Normalized coefficients c_i for the sphere (clear symbols) and the ellipsoid (filled symbols).



(a) Coefficients c_1 (circles) and c_2 (squares). (b) Coefficients c_3 (triangles)



(a) Coefficients t_1 (circles), t_2 (squares) and t_3 (triangles). (b) Coefficients s_1 (circles) and s_2 (squares)

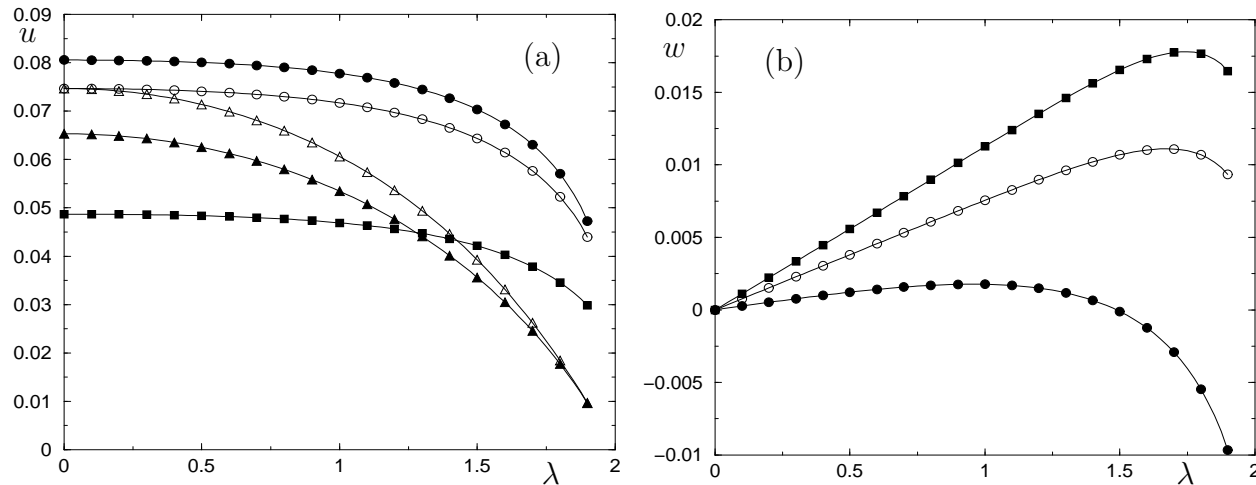
Settling normalized translational and angular velocities

Setting $U'_s = (\rho_s - \rho)a^2g/\mu$ one gets

(i) If $\mathbf{g} = g\mathbf{e}_1$: $\mathbf{U} = U'_s u_1 \mathbf{e}_1$, $\mathbf{W} = aU'_s w_2 \mathbf{e}_2$

(ii) If $\mathbf{g} = g\mathbf{e}_2$: $\mathbf{U} = U'_s u_2 \mathbf{e}_2$, $\mathbf{W} = -aU'_s w_1 \mathbf{e}_1$

(iii) If $\mathbf{g} = g\mathbf{e}_3$: $\mathbf{U} = U'_s u_3 \mathbf{e}_3$, $\mathbf{W} = \mathbf{0}$



Normalized velocities for the sphere (clear symbols) and the ellipsoid (filled symbols).

(a) Translational velocities u_1 (circles), u_2 (squares) and u_3 (triangles).

(b) Angular velocities w_1 (circles) and w_2 (squares)

Concluding remarks

- A **new** approach based on a boundary-integral formulation
 - **Valid for arbitrarily-shaped** particles!
- Easy implementation and nicely retrieves for a spherical particle results obtained elsewhere using a quite different (bipolar coordinates) approach
- Two tested approaches resorting to the free-space Green tensor and the Green tensor complying with the no-slip condition on the motionless spherical cavity
- The second one makes it possible to solely mesh the particle surface and offers more accurate results
- Numerical results reveal that a particle behaviour is slightly sensitive to its shape
 - In future: cope with the challenging case of a collection of particles!